Occupational exposure assessment of magnetic fields generated by induction heating equipment—the role of spatial averaging

2012 Phys. Med. Biol. 57 5943

(http://iopscience.iop.org/0031-9155/57/19/5943)

IOP Publishing Physics in Medicine and Biology

Phys. Med. Biol. **57** (2012) 5943–5953 doi:10.1088/0031-9155/57/19/5943

Occupational exposure assessment of magnetic fields generated by induction heating equipment—the role of spatial averaging

Bor Kos[1,2], **Blaž Valič**[2], **Tadej Kotnik**[1] **and Peter Gajšek**[2,3]

[1] Laboratory of Biocybernetics, Faculty of Electrical Engineering, University of Ljubljana, Tržaška 25, SI-1000 Ljubljana, Slovenia
[2] Institute of Non-Ionizing Radiation, Pohorskega Bataljona 215, SI-1000 Ljubljana, Slovenia

E-mail: bor.kos@fe.uni-lj.si, blaz.valic@inis.si, tadej.kotnik@fe.uni-lj.si and peter.gajsek@inis.si

Received 16 April 2012, in final form 13 July 2012
Published 11 September 2012
Online at stacks.iop.org/PMB/57/5943

Abstract

Induction heating equipment is a source of strong and nonhomogeneous magnetic fields, which can exceed occupational reference levels. We investigated a case of an induction tempering tunnel furnace. Measurements of the emitted magnetic flux density (B) were performed during its operation and used to validate a numerical model of the furnace. This model was used to compute the values of B and the induced *in situ* electric field (E) for 15 different body positions relative to the source. For each body position, the computed B values were used to determine their maximum and average values, using six spatial averaging schemes (9–285 averaging points) and two averaging algorithms (arithmetic mean and quadratic mean). Maximum and average B values were compared to the ICNIRP reference level, and E values to the ICNIRP basic restriction. Our results show that in nonhomogeneous fields, the maximum B is an overly conservative predictor of overexposure, as it yields many false positives. The average B yielded fewer false positives, but as the number of averaging points increased, false negatives emerged. The most reliable averaging schemes were obtained for averaging over the torso with quadratic averaging, with no false negatives even for the maximum number of averaging points investigated.

(Some figures may appear in colour only in the online journal)

Introduction

Induction heating applications are very common in industrial processes, such as metal melting and refinement (Faerman *et al* 1997), as well as welding and hardening (Bayindir *et al* 2003).

[3] Author to whom any correspondence should be addressed.

They are also becoming more common in cooking, for both professional and domestic use (Acero *et al* 2010).

The fields used by induction heating equipment are alternating and can range in frequency from tens of Hz to hundreds of kHz (Bayindir *et al* 2003, Millan *et al* 2010). With the exception of the 50 and 60 Hz subrange of power line frequencies, this range is also among the least investigated in the scientific literature in terms of human exposure (Floderus *et al* 2002). Since the field strength required by induction heating applications is typically very high due to large power demands, from tens of kW to several MW (Floderus *et al* 2002), there is a significant possibility for fields exceeding the occupational reference levels as set out in the ICNIRP guidelines (ICNIRP 2010). With operations that require close proximity of a worker to a induction heating source, the worker is typically exposed to a highly nonhomogeneous field. When reference levels are exceeded, the ICNIRP guidelines, as well as the currently valid IEEE standards (IEEE 2006), require the determination of dosimetric quantities in the human body, and their comparison to the basic restriction. In the investigated frequency range, the most widely used reference level is the magnetic flux density (B) and the basic restriction of the *in situ* electric field (E), where the latter can only be determined non-invasively by means of numerical dosimetry (Bakker *et al* 2012, Hirata *et al* 2011), or by measurements on phantoms.

Numerical determination of dosimetric quantities in the human body is a complex task, and the most frequently used numerical methods all rely on staircasing (representation of curved surfaces by cubic voxels), resulting in the possibility of large errors. To reduce the staircasing errors, the ICNIRP guidelines recommend averaging over a volume of $2 \times 2 \times 2$ mm^3, or using the 99th percentile value when investigating the tissue-specific E. We have previously used the whole body 999th permille (Kos *et al* 2011), while others have successfully employed spatial averaging of tissue conductivities to reduce drastic conductivity changes at the intra-tissue and tissue–air boundaries (Laakso and Hirata 2012).

In this study, we investigated the role of spatial averaging in the measurements of magnetic fields in empty space for classification of human exposure (overexposure versus compliance). Such averaging has been suggested in the literature (Jokela 2007, ICNIRP 2010), but to the authors' best knowledge, no attempt has yet been made to compare different averaging schemes in their predictive power regarding the classification of exposures. Here, we perform a comparison of six such schemes with the results of numerical dosimetry computed in the body serving as a reference.

We present a case of an induction tempering tunnel furnace where workers perform quality control checks near the entrance of the tunnel. We report the measurements and numerical simulations of the generated stray B and numerical simulations of induced E in the human body. Finally, we discuss the application of spatial averaging of B for determination of compliance with exposure guidelines.

Materials and methods

Magnetic flux density measurements

We performed measurements of the magnetic flux density (B) generated by an induction tempering tunnel furnace using a calibrated ELT-400 instrument with the 100 cm^2 probe (both from Narda STS, Pfullingen, Germany). Spot measurements of B were performed using the instrument's RMS detection mode that has a flat frequency response. The total uncertainty of the measurement setup determined in the frequency range from 6 Hz to 320 kHz is 2.3 dB. The tempering tunnel operates at 10 kHz and consists of three turns of wire, each running

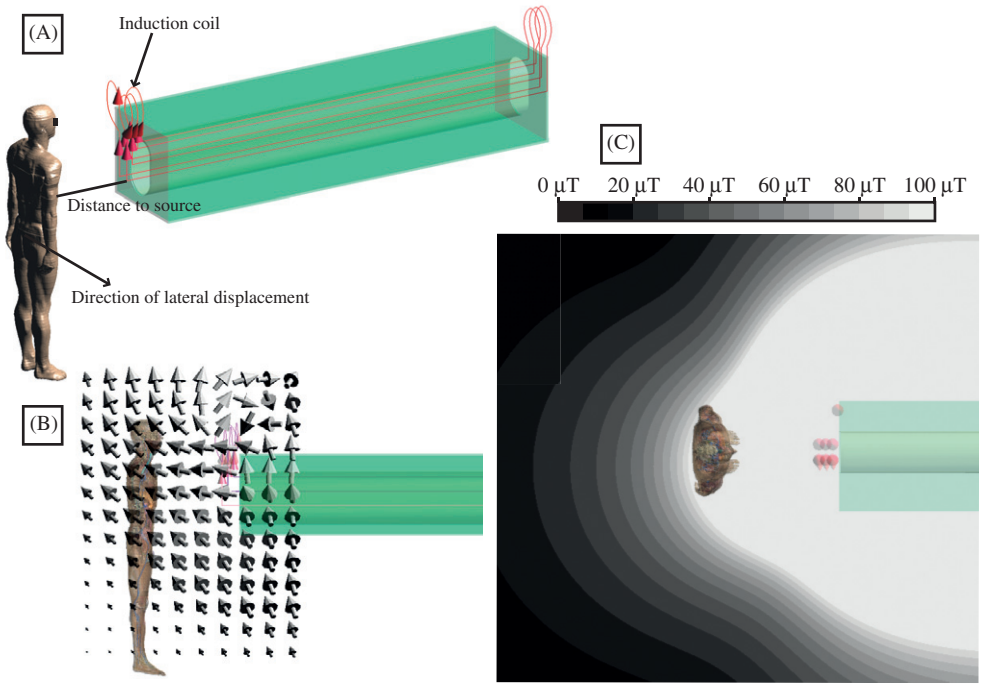

Figure 1. (A) Schematic view of the source geometry and positioning of the human model. The induction coil is composed of three turns carrying 2000 A of peak current. For the computations, the human model was positioned at five different distances to source and at three different lateral displacements. (B) Direction of the stray magnetic field. (C) Magnitude of the stray magnetic flux density. In all panels, the model is at 50 cm horizontal distance from the source.

horizontally around the tunnel 2.8 m long and 9 cm wide, and the adjacent turns separated vertically by 10 cm (figure 1(A)). The wires thus form a rectangular coil 3.06 m $\times$ 9 cm in cross-section (the wires extend some distance from the tunnel), with the magnetic field inside the coil generated predominantly in the vertical direction, and the stray magnetic field outside the furnace illustrated in figure 1(B).

The induction furnace is used for tempering hardened parts for drive shafts for the automotive industry. Due to the high precision and low tolerance of faulty parts required by automobile manufacturers, the parts undergo 100% inspection, which is done at the exit of the tempering tunnel to ensure any reject gets discarded as soon as possible in the manufacturing process. Additionally, due to space constraints for limiting factory floor footprint, the worker stations are positioned close to the source of the magnetic fields.

Numerical simulations

Using the SEMCAD X 14.6 software package (SPEAG, Zurich, Switzerland), a model of the source of magnetic field in the tunnel furnace was constructed based on the original manufacturer's technical drawings. The position and distance of the induction coil were determined with respect to the location where the quality control workers are typically stationed (figure 1). The model was then used to compute B in empty space at this location, as well as closer to the furnace. Since the probe used for magnetic-field measurements returned

Table 1. Body-averaging schemes in quantitative terms.

Averaging scheme	Back–front axis points	Right–left axis points	Vertical axis points	Total points
Whole body dense	3	5	19	285
Whole body reduced 1	1	3	10	30
Whole body reduced 2	1	3	5	15
Torso dense	3	5	11	165
Torso reduced 1	1	3	6	18
Torso reduced 2	1	3	3	9

B averaged over three orthogonal circular 100 cm^2 surfaces, we developed an algorithm that performs the same type of averaging on the numerical results to provide comparability between the measured and the numerically computed B. More precisely, B was computed in a sphere with a radius of 5.64 cm (in approx. 42 000 voxels), the normal B was averaged over three orthogonal cross sections, and the total average B was computed as the norm of its three-dimensional vector.

The numerical computations of *in situ* electric fields (E) were performed with the virtual family (Christ *et al* 2010) model 'Duke', i.e. the 34 year old male model. The model was positioned at a horizontal distance of 20, 30, 40, 50 or 100 cm from source (20 cm being the closest distance accessible to the workers in the case considered), and at a lateral displacement of 0, 20 or 50 cm to the right. The total number of different body positions was therefore 15. Vertically, the coil was positioned 120 cm above the feet of the model. Therefore, the area exposed to the highest B is the chest and head regions. The computation was performed at 10 kHz frequency using the low-frequency quasi-static solver implemented in SEMCAD X. Extended ($k = 2$) total uncertainty of the dosimetric simulations was estimated to be 4 dB with details on the estimation given in a previously published work (Kos *et al* 2011). The human model was discretized to $2 \times 2 \times 2$ mm^3 resolution, giving a total of 43 M-cells for the simulation. The resulting values of E were extracted for each tissue in the model (total of 77) and statistically analyzed to find their maximum, 99th percentile and mean values. We used the IT'IS database for dielectric properties of body tissues (Hasgall *et al* 2011).

Averaging algorithms

The ICNIRP guidelines (ICNIRP 2010) suggest that determining only the maximum value of B at a certain position can be an overly conservative measure for determining compliance with the exposure limits. Spatial averaging of fields over the whole body, or parts of the body, is suggested by Jokela (2007) to give a less conservative and more realistic estimate of actual exposure. We have investigated six different spatial averaging schemes by varying the number of averaging points. Averaging introduces the possibility of false negatives, i.e. situations where the worker is overexposed, yet the averaged fields are below the reference level. Since the main goal of reference levels is to prevent any possibility of overexposure, false negatives have to be avoided. On the other hand, false positives, where the averaged fields exceed the reference levels, while the actual exposure is below the basic restrictions, would imply that the averaging algorithm is overly conservative, albeit less conservative than the use of the spatial maximum value.

In total, six averaging schemes with varying number of averaging points (from 9 to 285 points) were investigated, as shown in table 1 and illustrated in figure 2. Thus, in the *whole body dense* scheme, the averaging was performed at 285 points forming a rectangular

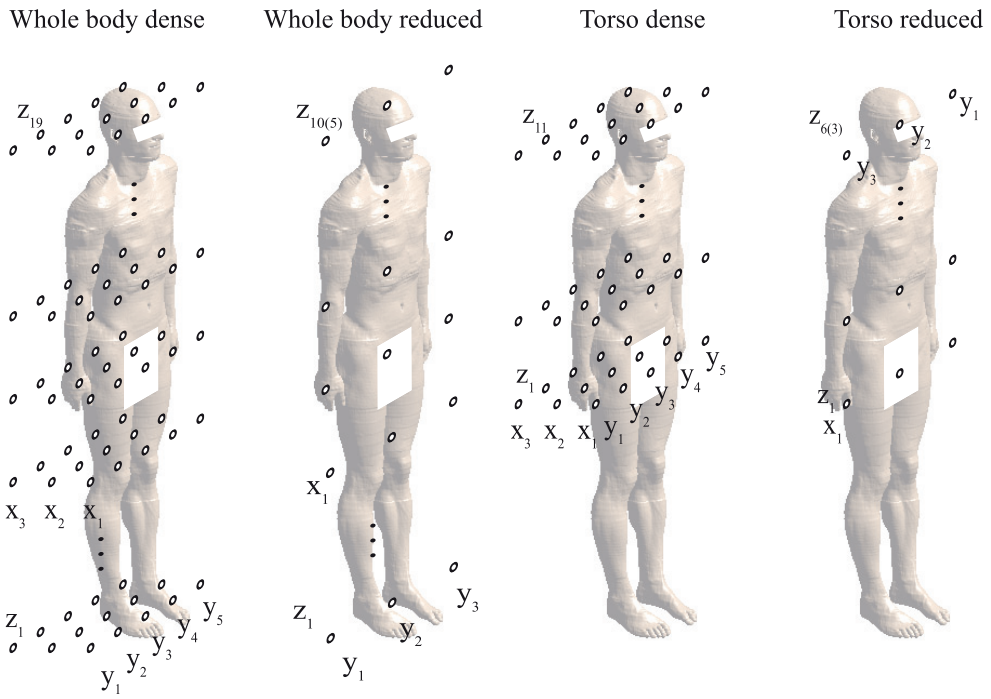

Figure 2. Body-averaging schemes illustrated. The whole body schemes covered the total body height of 180 cm, while the torso schemes covered only the 100 cm from the pelvis up. In the reduced schemes, the grid consisted of a single point along the front–back axis, located in the front plane of the body, since that plane is contributing the most to the total exposure.

grid with 3 points along the back–front (x) axis, 5 points along the right–left (y) axis, and 19 points along the vertical (z) axis, with all points spaced equidistantly in 10 cm intervals. The procedure was similar for the *torso dense* scheme, with the legs region excluded and thus only 11 points along the vertical axis. With the *whole body reduced 1* and *torso reduced 1* averaging schemes, the points were spaced at 20 cm intervals, while with both *reduced 2* schemes, they were spaced at 20 cm intervals horizontally and at 40 cm intervals vertically.

Although the practical use of averaging with a number of points as high as 285 or 165 is questionable without some sort of automated measurement system, it was included for comprehensiveness.

For each scheme, 15 different body positions were investigated. In addition, we also investigated the differences between a simple arithmetic mean and a quadratic mean in spatial averaging, with the quadratic mean defined as

$$B_{\text{average}} = \sqrt{\frac{1}{n}\sum_{i=1}^{n} B_i^2}$$

and thus giving more importance to higher values. This yielded a total of 180 investigated combinations of averaging scheme, type of mean and body position.

Table 2. Measured magnetic flux density at five points in front of the assessed induction furnace. The reference value of ICNIRP (2010) at 10 kHz is 100 μT.

Measurement spot	Measured B (μT)	Computed B (μT)	% error
1	350	224	−36%
2	117	70.5	−40%
3	116	176	52%
4	45	40.6	−10%
5	17	20	18%

Results and discussion

Measurements of magnetic flux density

The magnetic flux density (B) was measured at five points in front of the tempering tunnel during its operation. As shown in table 2, at three of these points, the measured values of B exceeded the ICNIRP guidelines (ICNIRP 2010). Since workers need to perform some tasks at the points where an excessive field has been measured, according to these guidelines a more detailed assessment—dosimetric evaluation of *in situ* induced electric field (E)—needs to be performed.

In table 2, we also compare the measured and the computed values of B at the locations corresponding to the measurement points. Although some of the errors are relatively large, they are still within the uncertainty boundaries as specified by Kuster *et al* (2006). Therefore, it is appropriate to use the computed values of B for the investigation of the influence of spatial averaging.

Numerical computation of magnetic flux density and in situ electric fields

The computed maximum and averaged fields at all investigated combinations of averaging scheme, type of mean and body position are shown in table 3, while a summary of the numerical dosimetry data is given in table 4. In our results, where the maximum B in the body does not exceed the ICNRIP reference levels, there are no cases of exposure exceeding the ICNIRP basic restrictions as indicated by the 99th percentile of E. Although Bakker *et al* (2012) have found some cases where such overexposure could occur, those were with child models exposed to homogeneous fields at the occupational reference levels. On the other hand, the maximum B yields many false positives and is thus an overly conservative predictor of overexposure, which is in agreement with the suggestions of the ICNIRP guidelines.

From the cross-referencing of tables 3 and 4, it is possible to identify the false negatives, i.e. the locations where the average B is below the reference level, while the induced E is above the basic restriction. There were three such false negatives in the 180 combinations investigated: at 40 cm distance in the aligned and 20 cm to-the-right positions, and at 20 cm distance in the 50 cm to-the-right position; all these false negatives were obtained using the whole-body-dense averaging scheme with the arithmetic mean. This indicates that whole-body averaging is inappropriate, particularly in highly nonhomogeneous fields.

Additionally, there were 17 false positives, with several locations where false positives were yielded only by the quadratic mean averaging, but not by the arithmetic mean. This is an expected result since the quadratic mean is more conservative, with the higher values given more importance.

Table 3. Computed values of averaged (*A*—arithmetic; *Q*—quadratic mean) and maximum (*M*) magnetic flux density (in μT). Since the occupational reference level at 10 kHz is exactly 100 μT, the numerical value of magnetic flux density is equal to the percentage of the reference level. The top row indicates the distances from the source to the frontal plane of the human body. Note that the maximum *B* values are the same in the aligned and 0.2 m right (R) position because the two positions share some measurement points which are located in the area with the strongest fields.

		Horizontal distance from source														
		20 cm			30 cm			40 cm			50 cm			100 cm		
Scheme	Lateral position	*A*	*Q*	*M*	*A*	*Q*	*M*	*A*	*Q*	*M*	*A*	*Q*	*M*	*A*	*Q*	*M*
	Aligned	190	291	1114	122	169	530	85	110	297	64	78	187	24	25	43
Whole body dense	0.2 m R	165	257	1114	111	155	530	81	104	297	61	75	187	23	25	43
	0.5 m R	80	113	476	65	86	315	53	66	213	44	53	149	20	22	41
	Aligned	270	399	1114	164	225	530	111	142	297	80	98	187	27	29	43
Whole body reduced 1	0.2 m R	236	368	1114	150	209	530	104	135	297	76	94	187	27	29	43
	0.5 m R	103	154	476	81	113	315	65	84	213	52	65	149	23	25	41
	Aligned	284	390	830	177	229	445	120	148	266	86	102	174	28	30	42
Whole body reduced 2	0.2 m R	249	359	830	161	214	445	112	141	266	83	99	174	28	30	42
	0.5 m R	111	157	400	83	115	279	66	87	196	53	67	141	23	25	40
	Aligned	302	381	1114	187	220	530	127	142	297	92	100	187	30	31	43
Torso dense	0.2 m R	261	337	1114	171	202	530	120	135	297	89	96	187	30	31	43
	0.5 m R	120	146	476	95	111	315	75	85	213	61	67	149	26	26	41
	Aligned	426	514	1114	253	289	530	165	182	297	116	124	187	35	35	43
Torso reduced 1	0.2 m R	371	474	1114	229	269	530	155	173	297	111	120	187	35	35	43
	0.5 m R	154	197	476	119	144	315	93	107	213	74	82	149	29	30	41
	Aligned	446	502	830	270	294	445	177	189	266	124	130	174	36	37	42
Torso reduced 2	0.2 m R	389	462	830	245	275	445	166	179	266	119	125	174	36	36	42
	0.5 m R	165	201	400	128	150	279	100	112	196	79	86	141	30	31	40

Table 4. Number of tissues with the 99th percentile of *in situ* electric field ($E_{99\%}$) exceeding the basic restriction (BR), the highest of the $E_{99\%}$ among all tissues, and its ratio to BR. The basic restriction at 10 kHz is 2.7 V m^{-1} for all tissues of the head and body (ICNIRP 2010).

Distance (m)		0.2	0.3	0.4	0.5	1
Aligned	No of tissues over BR	33	12	2	0	0
	max $E_{99\%}$	11.9 V m^{-1}	6.07 V m^{-1}	3.53 V m^{-1}	2.23 V m^{-1}	0.585 V m^{-1}
	max $E_{99\%}$/BR	439%	225%	131%	83%	22%
	Tissue with max $E_{99\%}$	Ear skin	Ear skin	Ear skin	Ear skin	Adrenal gland
0.2 m right	No of tissues over BR	28	10	1	0	0
	max $E_{99\%}$	8.45 V m^{-1}	4.63 V m^{-1}	3.00 V m^{-1}	2.10 V m^{-1}	0.616 V m^{-1}
	max $E_{99\%}$/BR	313%	172%	111%	78%	23%
	Tissue with max $E_{99\%}$	Mucosa	Mucosa	Mucosa	Mucosa	Bone
0.5 m right	No of tissues over BR	3	0	0	0	0
	max $E_{99\%}$	3.18 V m^{-1}	2.49 V m^{-1}	1.91 V m^{-1}	1.48 V m^{-1}	0.536 V m^{-1}
	max $E_{99\%}$/BR	118%	92%	71%	55%	20%
	Tissue with max $E_{99\%}$	Teeth	Mucosa	Mucosa	Mucosa	Bone

Table 4 also shows that the most overexposed tissues include mucosa, ear skin, bones and teeth. In this context, it should be noted that the restrictive ICNIRP limits aim to avoid stimulatory phenomena in the heart and the central nervous system, so overexposure of less susceptible tissues should not necessarily be viewed as a source of concern. Still, at the closest distance, the overexposed tissues also include white and gray matter, heart muscle and spinal cord.

All the results presented in tables 3 and 4 were obtained with the current of 2000 A flowing in the induction coil. However, this current can be adjusted to the needs of the particular manufacturing process, resulting in proportionally changed values of B and consequently of E. This can affect the assessment of exposure, including the occurrence of false negatives and positives. To emulate the changes of induction coil current, we have scaled the values of B as given in table 3, and the resulting values of E as given in table 4, by factors ranging from 0.1 to 3 in increments of 0.1, and again compared the 99th percentile of E to the basic restrictions. Thus, we have investigated a total of 30 different power levels and corresponding changes of B and E. The total number of misclassifications was determined for each normalization factor, and the results are summarized with respect to the averaging scheme in figure 3, which suggests that irrespective of magnetic flux density, the quadratic averaging scheme generally produces the fewest false negatives.

Table 3 and figure 3 also show that in both arithmetic and quadratic averaging, as the number of averaging points increased, false negatives emerged and increased in number. The most reliable averaging schemes were obtained for averaging over the torso with quadratic averaging, with no false negatives even for the maximum number of averaging points investigated.

Figure 4 shows the data on misclassifications with respect to the scaling factor. This figure highlights that field averaging is the most important for the range of magnetic flux densities that induce *in situ* electric fields close (either below or above) to the basic restriction. For scaling factors below 0.3, the basic restriction is not exceeded in any tissue for any of the analyzed body positions, while above 1.9, the basic restriction is exceeded in at least one tissue for each body position except at the largest (100 cm) distance from the induction tunnel. As a consequence, for these scaling factors the number of misclassifications is very small, implying that for either sufficiently low or sufficiently high B, averaging can be avoided. In addition, averaging also becomes unnecessary at distances over 1 m from the tunnel, where B

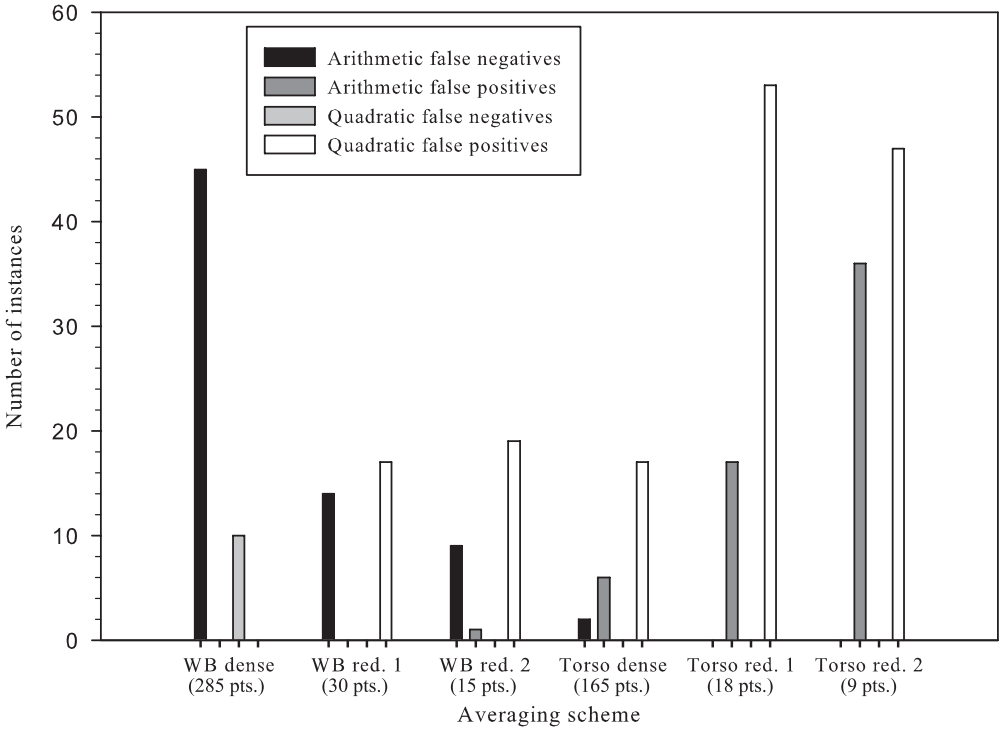

Figure 3. Misclassifications of exposure in different averaging schemes for the whole range of investigated scaling factors. The maximum B yielded 88 false positives and no false negatives.

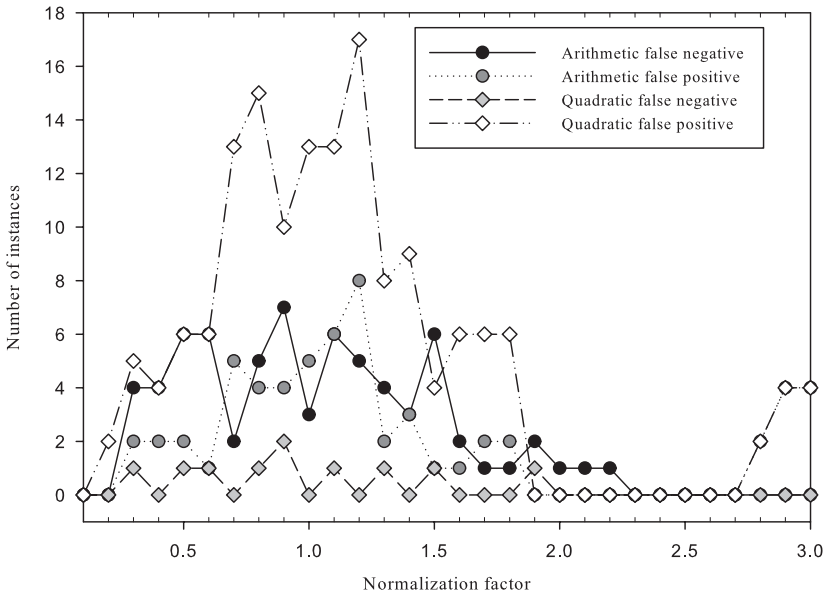

Figure 4. Misclassifications of exposure as functions of the scaling factor.

becomes almost homogeneous, and its maximum value can be taken as a reliable indicator of exposure.

The case studied here is in some aspects quite specific, as it considers a single-source-type functioning at a single frequency. However, as can be seen in figures 1(B) and (C), the magnetic field in the location of the human body is rather similar, both in the aspect of its spatial distribution and its nonhomogeneity, to those in front of typical circular coils. In our case, we did not investigate the very nonhomogeneous fields at extremely close distances to the furnace, as such distances are in practice inaccessible to the workers; this may not be the case in many other magnetic field sources, for which the situation, including reasonable averaging methods, should be addressed by a separate study. The same conclusion applies for sources operating at considerably higher or lower frequencies.

Conclusions

Magnetic fields generated by industrial induction furnaces can induce *in situ* electric fields exceeding the basic restriction according to the ICNIRP guidelines. For determination of occupational exposure, spatial averaging provides an adequate estimate, in the sense that it is protective, yet less conservative than the maximum value, which can lead to an excessive number of false positives. Quadratic averaging has a much lower likelihood of producing false negatives than simple arithmetic averaging, and averaging over the torso yields fewer false negatives than averaging over the whole body. Averaging is most important for magnetic fields that induce *in situ* electric fields close to the basic restriction, while for both significantly weaker or stronger fields the maximum value is a reliable indicator of exposure.

Acknowledgment

This work was supported by the Slovenian Research Agency under grant number L7-2231.

References

Acero J, Burdio J M, Barragan L A, Navarro D, Alonso R, Ramon J, Monterde F, Hernandez P, Llorente S and Garde I 2010 Domestic induction appliances *IEEE Ind. Appl. Mag.* **16** 39–47

Bakker J F, Paulides M M, Neufeld E, Christ A, Chen X L, Kuster N and van Rhoon G C 2012 Children and adults exposed to low-frequency magnetic fields at the ICNIRP reference levels: theoretical assessment of the induced electric fields *Phys. Med. Biol.* **57** 1815–29

Bayindir N, Kukrer O and Yakup M 2003 DSP-based PLL-controlled 50–100 kHz 20 kW high-frequency induction heating system for surface hardening and welding applications RID B-4867–2008 *IEE Proc. B* **150** 365–71

Christ A *et al* 2010 The Virtual Family—development of surface-based anatomical models of two adults and two children for dosimetric simulations *Phys. Med. Biol.* **55** N23–38

Faerman L, Luzgin V, Petrov A and Rachkov S 1997 Highly efficient induction heating units for metallurgy and machine construction *Metallurgist* **41** 191–3

Floderus B, Stenlund C and Carlgren F 2002 Occupational exposures to high frequency electromagnetic fields in the intermediate range (>300 Hz–10 MHz) *Bioelectromagnetics* **23** 568–77

Hasgall P, Neufeld E, Gosselin M, Klingenböck A and Kuster N 2011 IT'IS Database for thermal and electromagnetic parameters of biological tissues www.itis.ethz.ch/database

Hirata A, Takano Y, Fujiwara O, Dovan T and Kavet R 2011 An electric field induced in the retina and brain at threshold magnetic flux density causing magnetophosphenes *Phys. Med. Biol.* **56** 4091–101

ICNIRP 2010 Guidelines for limiting exposure to time-varying electric and magnetic fields (1 Hz to 100 kHz) *Health Phys.* **99** 818–36

IEEE 2006 IEEE standard for safety levels with respect to human exposure to radio frequency electromagnetic fields, 3 kHz to 300 GHz *IEEE Standard C95.1–2005 (Revision of IEEE Standard C95.1–1991)* doi:10.1109/IEEESTD.2006.99501

Jokela K 2007 Assessment of complex EMF exposure situations including inhomogeneous field distribution *Health Phys.* **92** 531–40

Kos B, Valič B, Miklavčič D, Kotnik T and Gajšek P 2011 Pre- and post-natal exposure of children to EMF generated by domestic induction cookers *Phys. Med. Biol.* **56** 6149–60

Kuster N, Torres V B, Nikoloski N, Frauscher M and Kainz W 2006 Methodology of detailed dosimetry and treatment of uncertainty and variations for *in vivo* studies *Bioelectromagnetics* **27** 378–91

Laakso I and Hirata A 2012 Reducing the staircasing error in computational dosimetry of low-frequency electromagnetic fields *Phys. Med. Biol.* **57** N25–34

Millan I, Burdio J M, Acero J, Lucia O and Palacios D 2010 Resonant inverter topologies for three concentric planar windings applied to domestic induction heating *Electron. Lett.* **46** 1225–6